

Network NOMA for Co-existence of Aerial and Terrestrial Users

Wee Kiat New¹, Chee Yen Leow¹, Keivan Navaie², and Zhiguo Ding³

¹Wireless Communication Centre, Universiti Teknologi Malaysia, Johor, Malaysia.

²Department of Computing and Communications, Lancaster University, Lancaster, UK.

³School of Electrical and Electronic Engineering, The University of Manchester, Manchester, UK.

Email: {weekiat@graduate, bruceleow@fke}.utm.my, k.navaie@lancaster.ac.uk, zhiguo.ding@manchester.ac.uk

Abstract—Scarcity of the radio spectrum and high inter-cell interference (ICI) are major impediments to efficient connectivity in cellular-connected unmanned aerial vehicles (UAV)s. To address these issues, we propose aerial-terrestrial network non-orthogonal multiple access (ATN-NOMA). In the proposed scheme, we pair the aerial user (AU) and terrestrial user (TU) in a NOMA setting to leverage their asymmetric channel gains and rate demands in downlink communication. The high ICI issue at the AU receiver is further managed by equipping the AU with an adjustable beamwidth directional antenna and forming a distributed beamforming among the coordinated terrestrial base stations (BSs). The proposed ATN-NOMA scheme obtains the optimal beamwidth and power allocation to maximize the TUs' sum-rate subject to the AU's Quality-of-Service (QoS) requirement. The corresponding optimization is a non-convex optimization problem for which we exploit the structure of the problem to obtain a local optimal solution. We further compare TUs' sum-rate and AU's outage probability of the proposed scheme with multiple schemes. Simulation results show that our proposed scheme significantly outperforms the existing schemes and further demonstrate a robust performance against UAV altitude variations.

I. INTRODUCTION

Unmanned aerial vehicles (UAV)s have gained significant interests in civil applications such as agriculture, construction, and delivery. To enable beyond-visual line-of-sight operation, the idea of connecting the UAVs as aerial users (AU)s to the cellular networks, also known as cellular-connected UAVs, has been proposed [1]. The co-existence of AUs and terrestrial users (TU)s, however, introduces new challenges and one of the key challenges is high level of inter-cell interference (ICI) at the AUs.

As discussed in [2], AUs that are hovering at a high altitude do not only establish LOS links with their associated terrestrial base station (BS) instead they also establish LOS links with other unintended terrestrial BS. This causes severe ICI at the AUs. Due to strong aerial links, the ICI at the AUs might then become more severe than that of the TUs located at the cell-edge.

Various approaches have been investigated in the literature [3], [4], however, existing works focus on orthogonal multiple access (OMA), where the spectral efficiency and number of concurrent connectivity are limited as each orthogonal resource block (RB) can only be assigned to a single user.

To overcome these limitations, the non-orthogonal multiple access (NOMA) can be employed. By leveraging the superposition coding at the transmitter and successive interference cancellation (SIC) at the receiver, NOMA allows multiple users to share the same RB. This enhances the spectral efficiency and enables massive connectivity.

Nevertheless, direct application of NOMA does not solve the ICI problem in aerial-terrestrial networks since using NOMA in multi-cell networks is also challenged by the ICI problem. Although several schemes have been proposed to address the ICI problem of the cell-edge users (e.g., [5]), the severe ICI problem at the AU in the multi-cell NOMA networks remains to be addressed.

Motivated by the above, we propose an aerial-terrestrial Network NOMA (ATN-NOMA) scheme. Inspired by [6], we propose the use of a directional antenna with adjustable beamwidth at the AU receiver. The use of a directional antenna with adjustable beamwidth has been applied in various applications such as satellite communication and remote sensing. Furthermore, we propose to employ Network NOMA [7], so that the distributed beamforming can be used to guarantee a reliable communication to the AU. Unlike existing schemes, the proposed ATN-NOMA scheme, which includes efficient receiving and transmitting strategies, can free the AU from ICI with a small number of coordinated BSs.

In this paper, we consider the downlink multi-cell networks with the co-existence of an AU and multiple TUs to evaluate the efficiency of the proposed scheme. The objective of the proposed ATN-NOMA scheme is to serve the TUs efficiently while reliable connectivity to the AU is prioritized. Since the control link is directly related to the safe operation of the UAV, a corresponding QoS requirement is imposed. We then investigate the maximum sum-rate of the TUs subject to the AU's QoS requirement. The major contributions of this paper are summarized as follows.

- We propose a novel ATN-NOMA scheme for the co-existence of AU and TUs. Specifically, we pair the AU and TUs to exploit their asymmetric channel and rate demand characteristics. In our proposed scheme, we employ directional antenna with adjustable beamwidth at the AU and Network NOMA to effectively mitigate the severe ICI at the AU.

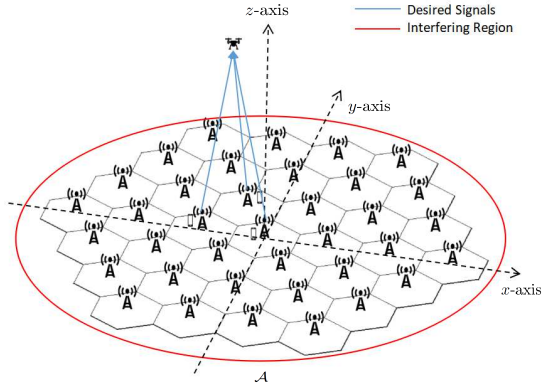


Figure 1. A schematic of a downlink multi-cell network with AU and TUs.

- We formulate an optimization problem to maximize the sum-rate of the TUs by optimal beamwidth and power allocation subject to the AU's QoS requirement. We then obtain the solution to the non-convex optimization problem by exploiting the structure of the problem.
- Lastly, we provide the simulation results of the proposed ATN-NOMA scheme to show its superiority in terms of TUs' sum-rate and AU's outage probability over existing schemes.

The rest of the paper is organized as follows: Section II details the system model and the proposed scheme, and Section III presents the solution to maximize the sum-rate of the TUs subject to the AU's QoS requirement. The simulation results are provided in Section IV followed by the conclusions drawn in Section V.

II. SYSTEM MODEL AND THE PROPOSED SCHEME

We consider a downlink wireless communication system with multiple terrestrial BSs, cell-center TUs, and a single AU in the subregion \mathcal{A} (see, Fig. 1). We denote the subscript, u , as the AU, $t \in \mathcal{T} = \{1, \dots, T\}$ as the associated cell-center TUs, $b \in \mathcal{B} = \{1, \dots, B\}$ as the coordinated terrestrial BSs with $T = B > 1$, and $\mathcal{I} = \{B + 1, B + 2, \dots, I\}$ as the set of interfering terrestrial BSs.

For simplicity, we assume that the locations of the terrestrial BSs are distributed according to the hexagonal cellular structure with a radius of r_0 and a fixed height at z_b within a subregion \mathcal{A} . The locations of the associated cell-center TUs are distributed uniformly around their associated BS with a maximum distance of $\frac{r_0}{2}$ and a fixed height at z_t . Without loss of generality, we assume that the cell-center TU, $t \in \mathcal{T}$, is associated to the BS, $b \in \mathcal{B}$, if $t = b$, and the cell-center TU, $t \in \mathcal{T}$, is not associated to the BS, $b \in \mathcal{B}$, if $t \neq b$.

We denote $\mathbf{w}^{\text{AU}} = (x_u, y_u, z_u)$, $\mathbf{w}_t^{\text{TU}} = (x_t^{\text{TU}}, y_t^{\text{TU}}, z_t^{\text{TU}})$, and $\mathbf{w}_b^{\text{BS}} = (x_b^{\text{BS}}, y_b^{\text{BS}}, z_b^{\text{BS}})$ as the 3D location of the AU, TU t , and BS b , respectively. The distance between TU t and BS b is:

$$d_{b,t} = \|\mathbf{w}_t^{\text{TU}} - \mathbf{w}_b^{\text{BS}}\|, \quad (1)$$

and the distance between the AU and BS b is:

$$d_{b,u} = \|\mathbf{w}^{\text{AU}} - \mathbf{w}_b^{\text{BS}}\|. \quad (2)$$

Let $\hat{\mathbf{w}}_b^{\text{BS}} \triangleq (x_b^{\text{BS}}, y_b^{\text{BS}})$ and $\hat{\mathbf{w}}^{\text{AU}} \triangleq (x_u, y_u)$ be the 2D coordinates of the BS b and AU, respectively. Then, the horizontal distance between the AU and BS b is $\hat{d}_{b,u} = \|\hat{\mathbf{w}}^{\text{AU}} - \hat{\mathbf{w}}_b^{\text{BS}}\|$.

The aerial communication link between the AU and the BS b follows the probability LOS/NLOS. Denote $v \in \{\text{L}, \text{N}\}$ as the types of links, where, L, and, N, represent the LOS and NLOS links, respectively. The probability of LOS between the AU and BS b is:

$$p_{b,u}^{\text{L}}(\hat{d}_{b,u}, z_u) = -\varphi \cdot \exp(-\xi \cdot \phi_{b,u}) + \zeta. \quad (3)$$

In (3), $\phi_{b,u} \triangleq \tan^{-1}\left(\frac{z_u - z_b}{\hat{d}_{b,u}}\right)$ is the elevation angle between the AU and BS b , and φ , ξ and ζ are constant coefficients related to the communication environment. The probability of NLOS between the AU and BS b is $p_{b,u}^{\text{N}}(\hat{d}_{b,u}, z_u) = 1 - p_{b,u}^{\text{L}}(\hat{d}_{b,u}, z_u)$.

Given link type, v , the effective channel gain between the AU and BS b is:

$$|h_{b,u}^v(\Psi)|^2 = \Xi_{b,u}^v(\Psi) |\Omega_{b,u}^v|^2, \quad v \in \{\text{L}, \text{N}\}, \quad (4)$$

where $\Xi_{b,u}^v(\Psi) \triangleq \frac{E_u F G_u^{\text{rx}}(\Psi)}{d_{b,u}^{\alpha_v}}$, and $|\Omega_{b,u}^v|^2$ account for the large and small-scale fading effects, respectively. In large-scale fading, $\Xi_{b,u}^v(\Psi)$, E_u accounts for the sidelobe gain from the BS, $F = \left(\frac{4\pi f_c}{c}\right)^{-2}$ accounts for the attenuation loss at the operating frequency f_c , $G_u^{\text{rx}}(\Psi)$ is the receiving antenna gain at the AU with a particular beamwidth Ψ . In (4), α_v denotes the aerial pathloss exponents, and $|\Omega_{b,u}^v|^2 \sim \text{Gamma}(m_u^v, \theta_u^v)$.

The effective channel gain between the TU t and BS b is:

$$|h_{b,t}|^2 = \Xi_{b,t} |\Omega_{b,t}|^2. \quad (5)$$

In (5), $\Xi_{b,t} \triangleq \frac{E_t F G_t^{\text{rx}}}{d_{b,t}^{\alpha}}$, and $|\Omega_{b,t}|^2$ account for the large and small-scale fading effects, respectively. In the large-scale fading effect, $\Xi_{b,t}$, E_t accounts for the mainlobe gain from the BS, G_t^{rx} is the receiving antenna gain at the TU t , α is the terrestrial pathloss exponent, and $|\Omega_{b,t}|^2 \sim \text{Gamma}(m_t, \theta_t)$. We assume that the TUs are equipped with omni-directional antenna and thus $G_t^{\text{rx}} = 1, \forall t$. In practice, we have $\alpha \geq \alpha_{\text{N}} \geq \alpha_{\text{L}}$, and $m_u^{\text{L}} \geq m_u^{\text{N}} \geq m_t$.

Based on the unique characteristics of the aerial-terrestrial networks, we design efficient receiving and transmitting strategies. In this scheme, a directional antenna with adjustable beamwidth is implemented at the AU, where the antenna is pointed directly below the AU (i.e., $\hat{\mathbf{w}}^{\text{AU}}$). The azimuth and elevation half-power beamwidth are assumed equal and they are denoted by 2Ψ , where $\Psi \in (0, \frac{\pi}{2})$.

According to [8], (eq. 2.2-2.51), the antenna gain in the direction of (ψ_u^a, ψ_u^e) is:

$$G_u^{\text{rx}}(\Psi) = \begin{cases} \frac{G_{\text{ref}}}{\Psi^2}, & \text{if } 0 \leq \psi_u^a \leq \Psi, 0 \leq \psi_u^e \leq \Psi, \\ G_0 \approx 0, & \text{otherwise,} \end{cases} \quad (6)$$

where $G_{\text{ref}} \approx 2.2856$, G_0 denotes the antenna gain outside the beamwidth of the directional antenna, ψ_u^a and ψ_u^e are the azimuth and elevation angles at the AU, respectively.

For any given \mathbf{w}^{AU} , the receive coverage of the AU is:

$$\mathcal{K}(\Psi) = \left\{ \mathbf{w}_k \left| \begin{array}{l} x = (z_u - c_u) \tan \Psi \cos \psi, \\ y = (z_u - c_u) \tan \Psi \sin \psi, \\ z = c_u, c_u \in [0, z_u], \psi \in [0, 2\pi), \end{array} \right. \right\}, \quad (7)$$

where $\mathbf{w}_k = (x + x_u, y + y_u, z)$, the set $\mathcal{K}(\Psi)$ is a cone, \mathbf{w}^{AU} is the apex of the cone, $z_u \tan \Psi$ is the radius of the cone base, and z_u is the height of the cone.

In addition, we employ Network NOMA among the coordinated BSs. In the context of ATN-NOMA, each coordinated BS, $b \in \mathcal{B}$, pairs their associated cell-center TU t and the AU over the same RB. Here, we consider the pairing of cell-center TUs and AU, where the dimension of the user channels are different, leading to a more challenging problem. Due to the high-altitude, the AU becomes a common user among the coordinated BSs. Hence, each of the coordinated terrestrial BS, $b \in \mathcal{B}$, transmits the following signal to perform a distributed beamforming:

$$\tilde{S}_b = \frac{h_{b,u}^v(\Psi)^H}{|h_{b,u}^v(\Psi)|} \sqrt{\rho_{b,u} P_{\text{tx}} s_u} + \frac{h_{b,u}^v(\Psi)^H}{|h_{b,u}^v(\Psi)|} \sqrt{\rho_b P_{\text{tx}} s_b}, \quad (8)$$

where $\frac{h_{b,u}^v(\Psi)^H}{|h_{b,u}^v(\Psi)|}$ is the phase from the BS b to the AU and P_{tx} is the total transmit power at the BS. Note that, the cell-center TU t is associated to the BS b if $t = b$. Thus, $s_u \sim \text{CN}(0, 1)$ and $s_b \sim \text{CN}(0, 1)$ are circular symmetric complex Gaussian (CSCG) signals intended for the AU and the associated cell-center TU b , respectively. Besides, $\rho_{b,u}$ and ρ_b are the power coefficients assigned to the AU and the associated cell-center TU b , respectively, where $\rho_{b,u} + \rho_b \leq 1$.

Unlike the terrestrial cell-edge user, the AU experiences severe ICI from other BSs due to its high altitude. Therefore, the received signal at the AU is:

$$y_u^{\text{rx}} = \sum_{b \in \mathcal{B}} |h_{b,u}^v(\Psi)| \sqrt{\rho_{b,u} P_{\text{tx}} s_u} + |h_{b,u}^v(\Psi)| \sqrt{\rho_b P_{\text{tx}} s_b} + \underbrace{\sum_{b \in \mathcal{I}} |h_{b,u}^v(\Psi)| \sqrt{P_{\text{tx}} \tilde{S}_b}}_{\text{ICI term}} + \sigma_u, \quad (9)$$

where $\sigma_u \sim \text{CN}(0, \sigma_n^2)$ is the noise observed at the AU and σ_n^2 is the noise power level. In order to decode its own signal, the AU has to treat the $s_b, \forall b \in \mathcal{B}$, and $\tilde{S}_b, \forall b \in \mathcal{I}$, as noise.

Hence, the AU decodes its message directly with the following signal-to-interference-plus-noise ratio (SINR):

$$\text{SINR}_u = \frac{\sum_{b \in \mathcal{B}} N |h_{b,u}^v(\Psi)|^2 \rho_{b,u}}{\sum_{b \in \mathcal{B}} N |h_{b,u}^v(\Psi)|^2 \rho_b + \sum_{b \in \mathcal{I}} N |h_{b,u}^v(\Psi)|^2 + 1}, \quad (10)$$

where $N = \frac{P_{\text{tx}}}{B_w \sigma_n^2}$ is the normalized transmit signal-to-noise (SNR) power and B_w is the system bandwidth. The achievable rate of AU is therefore:

$$R_u = B_w \log(1 + \text{SINR}_u). \quad (11)$$

Due to the severe pathloss and multipath effects at the terrestrial platform, the signal observed by the cell-center TU t is:

$$y_t^{\text{rx}} = \frac{h_{b,u}^v(\Psi)^H \tilde{h}_{b,t}}{|h_{b,u}^v(\Psi)|} \sqrt{\rho_{b,u} P_{\text{tx}} s_u} + \frac{h_{b,u}^v(\Psi)^H \tilde{h}_{b,t}}{|h_{b,u}^v(\Psi)|} \sqrt{\rho_b P_{\text{tx}} s_b} + \sigma_t, \quad (12)$$

where $\tilde{h}_{b,t}$ is the complex channel tap from its associated BS b to the cell-center TU t such that $b = t$, and $\sigma_t \sim \text{CN}(0, \sigma_n^2)$ is the noise observed at t . Denote $h_{b,t} = \frac{h_{b,u}^v(\Psi)^H \tilde{h}_{b,t}}{|h_{b,u}^v(\Psi)|}$, then we can rewrite the received signal of TU t in (12) as follows:

$$y_t^{\text{rx}} = h_{b,t} \sqrt{\rho_{t,u} P_{\text{tx}} s_u} + h_{b,t} \sqrt{\rho_t P_{\text{tx}} s_t} + \sigma_t. \quad (13)$$

To decode its own message, the associated cell-center TU t carries out SIC by first removing the message to AU with the following SINR:

$$\text{SINR}_t^{(u)} = \frac{N |h_{b,t}|^2 \rho_{t,u}}{N |h_{b,t}|^2 \rho_t + 1}, \quad (14)$$

Following the principle of NOMA, the associated cell-center TU t decodes its own message with the following SINR:

$$\text{SINR}_t = N |h_{b,t}|^2 \rho_t. \quad (15)$$

The achievable rate of TU t is therefore:

$$R_t = B_w \log(1 + \text{SINR}_t). \quad (16)$$

III. AERIAL-NETWORK NOMA

The objective of ATN-NOMA is to efficiently serve the TUs' link and reliably support the AU's link. For this reason, we maximize the sum-rate of the cell-center TUs by optimal beamwidth and power allocation subject to the AU's QoS requirement. The optimization problem can be formulated as follows:

$$\max_{\Psi, \rho_{b,u}, \rho_b} \sum_{b \in \mathcal{B}} R_b, \quad (17a)$$

$$\text{s.t.} \quad R_u \geq R_{\min}, \quad (17b)$$

$$B_w \log(1 + \text{SINR}_b^{(u)}) \geq R_{\min}, \forall b \in \mathcal{B}, \quad (17c)$$

$$0 \leq \rho_b, 0 \leq \rho_{b,u}, \forall b \in \mathcal{B}, \quad (17d)$$

$$\rho_b + \rho_{b,u} \leq 1, \forall b \in \mathcal{B}, \quad (17e)$$

$$\mathbf{w}_b^{\text{BS}} \subseteq \mathcal{K}(\Psi), \forall b \in \mathcal{B}, \quad (17f)$$

where (17a) is the sum-rate of the cell-center TUs, constraint (17b) ensures the AU's QoS requirement is satisfied, (17c) ensures that each associated cell-center TU can decode the AU information successfully. In addition, (17d) ensures the power coefficients are non-negative, (17e) ensures the power allocation is feasible, and (17f) ensures the coordinated BSs are within the receiving coverage of the AU so that the ATN-NOMA can be performed. Note that, the formulation in (17) is expressed using the fact that the cell-center TU $t \in \mathcal{T}$ is associated to the BS $b \in \mathcal{B}$ if $t = b$.

Problem (17) is a non-convex optimization problem due to the constraint (17b). Moreover, the optimization variables are mutually coupled. To find the optimal solution, we exploit the structure of the problem. Note that (17a), (17c), (17d) and (17e) are independent of Ψ . To obtain the optimal beamwidth, we provide the following proposition:

Proposition 1. R_u is a non-increasing function of Ψ .

Proof: Substituting (4) and (6) into (11), yields

$$R_u = B_w \log \left(1 + \frac{\sum_{b \in \mathcal{B}} \frac{\Upsilon_b^v \rho_{b,u}}{\Psi^2}}{\sum_{b \in \mathcal{B}} \frac{\Upsilon_b^v \rho_b}{\Psi^2} + \sum_{b \in \mathcal{I}} \frac{\Upsilon_b^v}{\Psi^2} + 1} \right). \quad (18)$$

where $\Upsilon_b^v = \frac{NE_u F G_{ref} |\Omega_{u,v}|^2}{d_{b,u}^{\alpha_v}}$. Taking the derivative of R_u w.r.t. Ψ , we have:

$$\frac{\partial R_u}{\partial \Psi} = \frac{-2B_w \Psi \sum_{b \in \mathcal{B}} \Upsilon_b^v \rho_{b,u}}{\ln(2) c_1 \cdot c_2} \leq 0, \quad (19)$$

where $c_1 = \left(\Psi^2 + \sum_{b \in \mathcal{B}} \Upsilon_b^v (\rho_b + \rho_{b,u}) + \sum_{b \in \mathcal{I}} \Upsilon_b^v \right)$ and $c_2 = \left(\Psi^2 + \sum_{b \in \mathcal{B}} \Upsilon_b^v \rho_b + \sum_{b \in \mathcal{I}} \Upsilon_b^v \right)$. ■

Since (17a), (17c), (17d) and (17e) are independent of Ψ , and by proposition 1, R_u is a non-increasing function of Ψ , the optimal bandwidth Ψ in (17) can be obtained by solving the following optimization problem:

$$\min_{\Psi} \quad \Psi, \quad (20a)$$

$$\text{s.t.} \quad \hat{d}_{b,u} \leq (z_u - z_b) \tan \Psi, \quad \forall b \in \mathcal{B}. \quad (20b)$$

where (20b) geometrically ensures that the coordinated BSs are within the receiving coverage of the AU. Since $\tan \Psi$ is a strictly increasing function of Ψ over $\Psi \in (0, \frac{\pi}{2})$, the uniqueness of Ψ^* is guaranteed.

Given the optimal beamwidth Ψ^* , (17) is then reduced to:

Algorithm 1 Optimal Beamwidth and Power Allocation

- 1: **Input:** $N, |h_{b,u}^v(\Psi)|^2, B_w, R_{\min}$
 - 2: **Output:** $\Psi^*, \rho_{b,u}^*, \rho_b^*$
 - 3: Obtain Ψ^* by solving (20) via convex programming
 - 4: Obtain $\rho_{b,u}^*, \rho_b^*$ by solving (21) via CCP
 - 5: **end**
-

$$\max_{\rho_{b,u}, \rho_b} \quad \sum_{b \in \mathcal{B}} R_b, \quad (21a)$$

$$\text{s.t.} \quad f_1(\rho_{b,u}, \rho_b) - g_2(\rho_{b,u}) \geq \frac{R_{\min}}{B_w}, \quad (21b)$$

$$f_2(\rho_{b,u}, \rho_b) - g_2(\rho_b) \geq \frac{R_{\min}}{B_w}, \quad \forall b \in \mathcal{B}, \quad (21c)$$

$$0 \leq \rho_b \leq 1, 0 \leq \rho_{b,u} \leq 1, \quad \forall b \in \mathcal{B}, \quad (21d)$$

$$0 \leq \rho_b + \rho_{b,u} \leq 1, \quad \forall b \in \mathcal{B}, \quad (21e)$$

where

$$f_1(\rho_{b,u}, \rho_b) = \log \left(1 + \sum_{b \in \mathcal{B}} N |h_{b,u}^v(\Psi^*)|^2 (\rho_b + \rho_{b,u}) + I_{\text{tot}} \right),$$

$$g_2(\rho_{b,u}) = \log \left(1 + \sum_{b \in \mathcal{B}} N |h_{b,u}^v(\Psi^*)|^2 \rho_b + I_{\text{tot}} \right),$$

$$f_2(\rho_{b,u}, \rho_b) = \log \left(1 + N |h_{b,b}|^2 (\rho_b + \rho_{b,u}) \right),$$

$$g_2(\rho_b) = \log \left(1 + N |h_{b,b}|^2 \rho_b \right),$$

and $I_{\text{tot}} = N \sum_{b \in \mathcal{I}} |h_{b,u}^v(\Psi^*)|^2$ is the aggregated ICI. The local optimal solution of (21) can then be obtained via convex-concave procedure (CCP) [9]. The solution to (17) is shown in Algorithm 1.

IV. SIMULATION RESULTS

In this section, we provide the simulation results to evaluate the performance of our proposed ATN-NOMA scheme. In our simulations, we compare the performance of the following schemes:

- CoMP-OMA [3] with fixed beamwidth (FB-OMA),
- CoMP-OMA [3] with optimal beamwidth (OB-OMA),
- Network-NOMA with fixed power allocation [7] and fixed beamwidth (FB-FNOMA),
- Network-NOMA with fixed power allocation [7] and optimal beamwidth (OB-FNOMA),
- Network-NOMA with fixed beamwidth and optimal power allocation (FB-NOMA),

For OMA, we consider FDMA with equal bandwidth allocation to the AU and TUs. For the fixed beamwidth, we set $\Psi_f = \tan\left(\frac{2r_o}{81}\right)$ to ensure $\text{card}(\mathcal{B}) = 3$. For the Network-NOMA with fixed power allocation, we set $\rho_{b,u} = 0.9$ and

Table I
PARAMETER SETTINGS

Parameter	Value	Parameter	Value
P_{Tx}	26 dBm	f_c	2 GHz
B_w	180 KHz	r_0	500 m
σ_n^2	-174 dBm/Hz	(E_u, E_t)	(-3, 10) dB
R_{\min}	100 Kbps	(φ, ξ, ζ)	(1, .151, 1)
$\text{card}(\mathcal{B} \cup \mathcal{I}) \subseteq \mathcal{A}$	37	$(\alpha_L, \alpha_N, \alpha)$	(2.1, 3.7, 4)
$\text{card}(\mathcal{B})$	3	(m_u^L, m_u^N, m_t)	(3, 2, 1)
z_b, z_t	(19, 1.5) m	$(\theta_u^L, \theta_u^N, \theta_t)$	$(\frac{1}{3}, \frac{1}{2}, 1)$

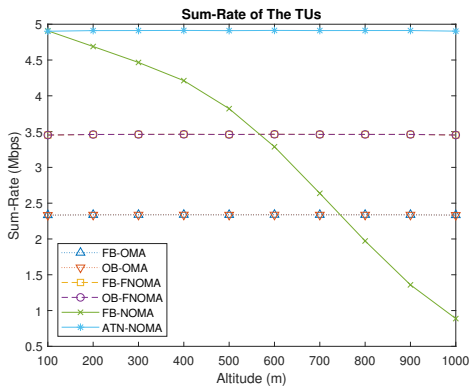


Figure 2. Sum-rate of the TUs

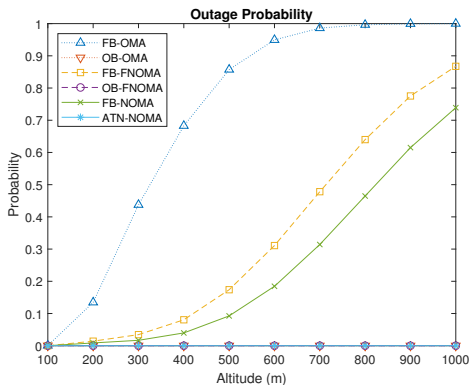


Figure 3. Outage Probability

$\rho_b = 0.1$ to compensate the ICI at the AU. The parameters used in the simulation are as shown in Table I.

Fig. 2 shows the sum-rate of the TUs over different altitudes. The proposed ATN-NOMA scheme achieves the highest sum-rate as compared to the other schemes. Specifically, the proposed ATN-NOMA achieves an average of 110% and 42% sum-rate improvement as compared to schemes based on OMA and FNOMA, respectively. This improvement is achieved due to the optimal beamwidth and power allocation, where the earlier and latter minimize the interference and required power at the AU.

Thanks to the spectrum sharing technique, schemes based on NOMA generally outperforms schemes based on OMA in terms of sum-rate. Furthermore, FB-OMA and OB-OMA achieve the same sum-rate because fixed resource allocation are given to the TUs regardless of the AU's performance. For the same reason, FB-FNOMA and OB-FNOMA achieve the same sum-rate. Although schemes based on optimal beamwidth and fixed beamwidth achieve the same sum-rate, they have vastly different impact on the outage probability of the AU.

Fig. 3 shows the outage probability over different altitudes. Results show that schemes based on optimal beamwidth achieve a much lower outage probability as compared to schemes based on fixed beamwidth. This is because, with the

optimal beamwidth, the ICI at the AU is mitigated for different altitudes. With a small number of coordinated BSs forming the distributed beamforming (e.g., $\text{card}(\mathcal{B}) = 3$ here), the AU is free from ICI. Due to the spectrum sharing technique, schemes based on NOMA also outperforms OMA in terms of outage probability. The combination of efficient receiving and transmitting strategies in the proposed ATN-NOMA scheme therefore delivers the best TUs' sum-rate and AU's outage probability as compared to existing schemes.

V. CONCLUSION

In this paper, we consider downlink multi-cell networks with the co-existence of AU and TUs. To ensure high spectral efficiency and massive connectivity, we proposed the ATN-NOMA scheme to support both the AU and TUs for control and data links, respectively. In the proposed ATN-NOMA scheme, a directional antenna with adjustable beamwidth is implemented at the AU and a distributed beamforming is performed by the coordinated BSs to mitigate the severe ICI problem at the AU. To guarantee the optimality of the proposed scheme, we maximized the sum-rate of the TUs by optimal beamwidth and power allocation subject to the AU's QoS requirement. Our simulation results showed that our proposed scheme significantly outperforms existing schemes in terms of sum-rate and outage probability, and further demonstrate a robust performance against UAV altitude variations.

ACKNOWLEDGMENT

This work was supported in part by H2020-MSCA-RISE-2015 under Grant ATOM 690750, in part by the Ministry of Education Malaysia under Grant 07085 and in part by the Universiti Teknologi Malaysia under Grant 19H58 and Grant 04G37.

REFERENCES

- [1] Y. Zeng, J. Lyu, and R. Zhang, "Cellular-Connected UAV: Potential, Challenges, and Promising Technologies," *IEEE Wireless Communications*, vol. 26, pp. 120–127, February 2019.
- [2] "Enhanced LTE Support for Aerial Vehicles-Release 15," tech. rep., 3rd Generation Partnership Project, 2017.
- [3] I. Kovacs, R. Amorim, H. C. Nguyen, J. Wigard, and P. Mogensen, "Interference Analysis for UAV Connectivity over LTE Using Aerial Radio Measurements," in *2017 IEEE 86th Vehicular Technology Conference (VTC-Fall)*, pp. 1–6, Sept 2017.
- [4] H. C. Nguyen and R. Amorim and J. Wigard and I. Z. Kovács and T. B. Sørensen and P. E. Mogensen, "How to Ensure Reliable Connectivity for Aerial Vehicles Over Cellular Networks," *IEEE Access*, vol. 6, pp. 12304–12317, 2018.
- [5] W. Shin, M. Vaezi, B. Lee, D. J. Love, J. Lee, and H. V. Poor, "Non-Orthogonal Multiple Access in Multi-Cell Networks: Theory, Performance, and Practical Challenges," *IEEE Communications Magazine*, vol. 55, pp. 176–183, Oct 2017.
- [6] H. He, S. Zhang, Y. Zeng, and R. Zhang, "Joint Altitude and Beamwidth Optimization for UAV-Enabled Multiuser Communications," *IEEE Communications Letters*, vol. 22, pp. 344–347, Feb 2018.
- [7] Y. Sun, Z. Ding, X. Dai, and G. K. Karagiannidis, "A Feasibility Study on Network NOMA," *IEEE Transactions on Communications*, vol. 66, pp. 4303–4317, Sep. 2018.
- [8] C. A. Balanis, *Antenna Theory: Analysis and Design, 3rd Edition*. John Wiley & sons, 2005.
- [9] T. Lipp and S. Boyd, "Variations and Extension of The Convex-Concave Procedure," *Optimization and Engineering*, vol. 17, no. 2, pp. 263–287, 2016.